www.s2is.org
International Journal on Smart Sensing and Intelligent Systems
ISSN 1178-5608

MULTI-SCALE COMPRESSED SENSING BASED ON SPLIT AUGMENTED LAGRANGIAN SHRINKAGE ALGORITHM FOR IMAGE SUPER-RESOLUTION RECONSTRUCTION

Tian Shu-yao [1,2] and Hu Chun-hai [1]
1School of Electrical Engineering, Yanshan University, Qinhuangdao, 066004, P.R. China
2School of Electromechanical, Hebei Normal University Of Science & Technology, Qinhuangdao, 066004, P.R. China
Emails: 514126299@qq.com

Submitted: Dec. 16, 2015 ***Accepted: Mar. 21, 2016*** ***Published: June 1, 2016***

Abstract- This paper proposes a multi-scale compressed sensing algorithm in shearlet domain by exploiting discrete Shearlet transform which can optimally represent the images with edges. An image is decomposed by shearlet. The compressed sensing is deployed in each of the directional sub-bands of high frequency scales. And inverse measurement matrix is modified by the upsampling operator to enhance the resolution of image. In addition, the original image reconstructed by compressed sensing based on super- resolution can produce the low subbands with high frequency. And an split augmented lagrangian shrinkage algorithm is exploited for compressed sensing image reconstruction , which can improve reconstruction image quality and convergence rate. Experimental results has shown that the proposed method can reconstruct the image with less iterative time by using fewer samples, improve the computational efficiency as well as achieve the images with high quality.

Index terms*: multi-scale compressed sensing, discrete Shearlet transform, super-resolution reconstruction algorithm, measurement matrix.*

Fund Project：The National Natural Science Fund，project number;：61201110

I. INTRODUCTION

Recently, the deployment of Compressed Sensing (CS) for the sampling and reconstruction of images has received growing attention [1]. It provides us a framework of simultaneously acquiring and compressing image data when in conventional imaging systems, digital images are acquired by Nyquist sampling[2] at a high rate and most of the sampling data are thrown away for the purpose of compression. The basic idea of CS is that an image, unknown but supposed to have a sparse representation in one known basis can be reconstructed from a small number of non-adaptive linear projections onto a second basis that is incoherent with the first via a tractable convex optimization program.

The theory derived in [3] shows that the multi-scale compressed sensing (MCS) scheme gets accuracy compared with linear sampling, with only fewer samples. Assume a signal decomposed into a baseband and a series of high passbands, CS is only applied to high passbands for reconstruction while the baseband retains the whole information during the transmission. Under the condition that a signal is sufficiently sparse in some basis, the recovery signal quality of MCS is far better that that of traditional CS. Based on image signals, James et.al proposed a block- partition- based MCS method by using wavelet transform as the image sparse representation. And Tsaig et.al proposed a Curvelets- based MCS method [4], which shows more sparsity in representation of images compared with the traditional wavelet transform. Thus, it is more ideal for the recovery signals quality in reference [4]. Since the discrete Shearlet transform (DST) [5]is regarded as the optimally sparse representation of signals, we developed a multi-scale compressed sensing in Shearlet domain (MCSS) to reconstruct the signals via fewer observations.

In practice, the spatial resolution of the optical system is restricted due to the limitation of energy consumption and transmission bandwidth. To overcome the above problems, by introducing the idea of single image super resolution [6], we designed a multi-scale compressed sensing in Shearlet- domain-based image super resolution fast reconstruction method (MCSS_SR). SR is image processing technology which can be described as to recover a high resolution (HR) image from one or more low resolution (LR) images[7].

In MCSS_SR approach, we first improve the measurement matrix by using the down-sampling and blur matrice to ensure that the modified matrix satisfies restricted isometry property (RIP)[8-10] , and apply it to the high passband of Shearlet domain to obtain the observations. In the processing of reconstruction, the wavelets are deployed in each directional subband to further increase the sparsity. The inverse measurement matrix includes the upsampling operation, so it can finally reconstruct HR image through split augmented lagrangian shrinkage algorithm(SALSA)[11]. The experimental results show that it is ideal for recovering images of MCSS_SR without overly increasing the complexity, which has the good effect on saving energy consumption of the front-end acquisition and transmission system bandwidth, and which is suitable for large scenes monitoring with limited energy, remote sensing imaging and other fields.

II. MCSS_SR METHOD CONSTRUCTION

The traditional CS theory shows that, if a signal $x \in R^N$ can be represented by a basis Ψ , that means it is K sparse in Ψ domain, then we choose a measurement matrix $\Phi \in R^{m \times N}$ satisfying the requirement of unrelated with Ψ and obtain the observations $y = \Phi x$ ($y \in R^m$. If the measurement time satisfies the expression: $m > C \cdot K \cdot \log(N)$, it is considered that Y contains sufficient information, and the original signal x can be reconstructed by solving the optimization problem ℓ : $\min\left\|\Psi^T \hat{x}\right\|_0 \ s.t.\ y = \Phi\Psi^T x$. Bcause the a ℓ optimization is a NP-hard problem, which is unable to be solved, we translate it into an equivalent and can solve ℓ norm optimization problem [5]: $\min\left\|\Psi^T \hat{x}\right\|_1 \ s.t.\ y = \Phi\Psi^T x$.

Whether the signal is sparse or not is the key of CS theory. Most of the natural images can be sparse representation according to the previous works. Existing methods of image multi-scale geometric analysis, such as the Shearlet transform proposed by Guo [12], associates geometry with multi-scale analysis according to affine systems, which can be implemented for “the most sparse” representation of images.

Easley, et al. [13] construct discrete Shearlet transform (DST), which combines Laplacian pyramid method with frequency directional filter bank (FDFB) defined in pseudo polar frequency domain frequency domain to represent the images. Because each of direction filters in FDFB meets the compactly supported property, it does not exist the spectrum aliasing phenomenon, meanwhile improve the direction selectivity. Figure 1 represents an example of FDFB (with six directional filters), dividing the frequency spectrum without leak in PPFC.

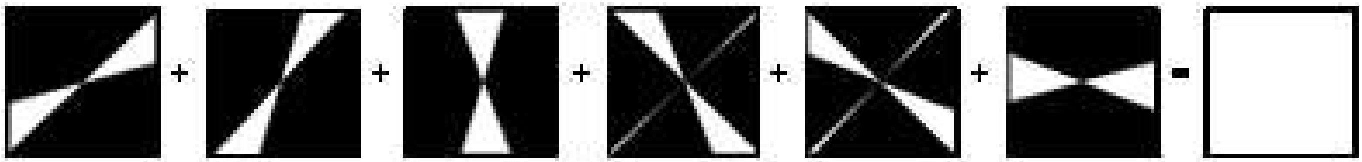

Figure.1 In PPFC, FDFB (with six directional filters) divides the frequency spectrum without leak

An image after the decomposition of DST can be represented as:

$$f = \beta_{j_0}\varphi_{j_0} + \sum_{j=j_0}^{J}\sum_{d}\alpha_{j,d}\phi_{j,d} \qquad (1)$$

φ_{j_0} , $\phi_{j,d}$ are the scaling coefficient function and Shearlet function respectively. We preserve the whole low frequency information β_{j_0} , for it contains most of image energy and is almost sparse, The direction subband of high frequency scale $\alpha_{j,d}$ describes edges and texture details of the image, which possessed strong sparsity. Taking advantage of this properties, we apply CS only to $\alpha_{j,d}$ and obtain:

$$y_{j,d} = \Phi_{j,d}\alpha_{j,d} \qquad (2)$$

And reconstruct information $\hat{\alpha}_{j,d}$ is obtained by solving ℓ norm optimization problem .

$$\min\left\|\hat{\alpha}_{j,d}\right\|_1 \; s.t. \; y_{j,d} = \Phi_{j,d}\alpha_{j,d} \qquad (3)$$

And the final image is recovered by MCSS method, $\hat{f} = \beta_{j_0}\varphi_{j_0} + \sum_{j=j_0}^{J}\sum_{d}\hat{\alpha}_{j,d}\phi_{j,d}$.

Suppose that the size of an original image of high frequency is $LN_1 \times LN_2$, and we put a downsampling matrix D on it; assume the sampling factor as L , then we get the low frequency image, the size of which is $N_1 \times N_2$. Then the observation matrix is $\tilde{\Phi}$. In order to ensure $\tilde{\Phi}$ subject to RIP conditions, Φ is specified as the local Hadamard matrix.

The local hadamard measurement matrix proposed by Do [14] can accelerate the operation and reduce the storage space reconstruction algorithm. Its expression is as follows:

$$\Phi = Q_M W_B P_N \qquad (4)$$

W_B is a diagonal matrix composed by the block matrix B , P_N is a random scrambling matrix and the function is to scramble the input signal to make sure it is uncorrelated with the Φ . Q_M represents the operation factor of M lines from N dimensions coefficients. The effect of scrambling P_N to ensure that $\tilde{\Phi}$ is still subject to RIP condition and can be chosen as the observation matrix of MCSS_SR method.

Based on the Reference [14], assume the measurement number is m ($m \ge K\sqrt{N/B}\left(\log N\right)^2$, B is the block dimension, N is the image dimension, K represents K non-zeros coefficients in the sparse signal), the local Hadamard matrix can accurately reconstruct the signal with great probability. In MCSS_SR, suppose that the sampling factor is n , so that the original image can be accurately reconstructed, $m/n \ge C \cdot K \cdot \sqrt{N/B} \cdot \left(\log N\right)^2$, which means the measurement times of $\tilde{\Phi}$ is $m \ge C \cdot n \cdot K \cdot \sqrt{N/B} \cdot \left(\log N\right)^2$

III MCSS_SR RECONSTRUCTION BY ITERATIVE HARD THRESHOLD ALGORITHM

The CS reconstruction algorithms are mainly based on basis pursuit algorithm (BP) [15], the matching pursuit algorithm (MP) [16] and iterative hard threshold algorithm (iterated hard shrinkage, IHT) [17]. In order to solve the problem of reconstruction algorithm convergence speed, reference[11] proposed split augmented lagrangian shrinkage algorithm(SALSA). the basic idea of SALSA is that using a variable splitting to obtain an equivalent constrained optimization formulation, which is then addressed with an augmented lagrangian method. The proposed algorithm is an instance of the so-called alternating direction method of multipliers, for which convergence has been proved. In MCSS_SR, we consider the SALSA as reconstruction algorithm to speed up convergence. Moreover, a context model based spatial adaptive soft threshold method is introduced to the traditional SALSA algorithm, which can preserve more details in the process of the reconstruction. The original low resolution image $Y \in R^N$ decomposed by DST gets its Shearlet coefficients, which can be expressed as:

$$Y = \beta_{j_0}^{(Y)}\varphi_{j_0} + \sum_{j=j_0}^{J}\sum_{d}\alpha_{j,d}^{(Y)}\phi_{j,d} \tag{5}$$

To improve the spatial resolution of $\beta_{j_0}^{(Y)}$, Y is regarded as CS measurements of the corresponding high-resolution images of X, and the measurement matrix is $\Phi = DH$,where D , H are the down-sampling operator and blur operator respectively. X can be sparse represented by wavelets: $X = \Psi\alpha$. Reference [18] proved that for an image of 512×512, the correlation degree is $\mu(\Phi,\Psi)=158.3$ .The X dimension $N^{(X)} = 4N$, it can be accurately reconstructed X_{CS} in the following equation:

$$\min\|\hat{\alpha}\|_1 \ s.t.\ Y = \Phi\Psi\alpha = DH\Psi\alpha \tag{6}$$

And X_{CS} is obtained by solving the equation $X_{CS} = \Psi\hat{\alpha}$. After being decomposed by DST again, X_{CS} can be expressed as:

$$X_{cs} = \beta_{j_0}^{(X_{CS})}\varphi_{j_0} + \sum_{j=j_0}^{J}\sum_{d}\alpha_{j,d}^{(X_{CS})}\phi_{j,d} \tag{7}$$

$\beta_{j_0}^{(X_{CS})}$ is the low information of X_{MCSS_SR} . To reconstruct $\alpha_{j,d}^{(Y)}$, we apply $\alpha_{j,d}^{(X_{CS})}$ as the iteration initial value, and exploit $\tilde{\mathbf{\Phi}}$ to CS. In order to further strengthen the sparsity of subbands, we exploit the wavelets Ψ_w^T as the sparse representation to $\alpha_{j,d}^{(X)}$, and solve the ℓ_1 norm optimization problem by SALSA algorithm:

$$\min\left\|\Psi_w^T\hat{\alpha}_{j,d}^{(X)}\right\|_1 \ s.t.\ y_{j,d}^{(Y)} = \tilde{\Phi}_{j,d}\Psi_w^T\hat{\alpha}_{j,d}^{(X)} \tag{8}$$

$y_{j,d}^{(Y)} = \Phi_{j,d}\alpha_{j,d}^{(Y)}$,To ensure $\Psi_w^T\hat{\alpha}_{j,d}^{(X)}$ can be reconstructed by $y_{j,d}^{(Y)}$ .Assume $\Psi_w^T\hat{\alpha}_{j,d}^{(X)}$ is K' sparse, the measurement times m should satisfy： $m \ge C\cdot n\cdot K'\cdot\sqrt{N_j/B}\cdot(\log N_j)^2$, N_j is the j scale dimension of HR image.

The basic idea of SALSA is that using a variable splitting to obtain an equivalent constrained optimization formulation, which is then addressed with an augmented Lagrangian method. And the optimal solution meets:

$$\min_{x\in R^N}\frac{1}{2}\|y-\Phi x\|_2^2 + \tau\|\Psi x\|_1 \tag{9}$$

$x\in R^N$, x is the original image, Φ is the measurement matrix， Ψ is the transform domain， $y\in R^N$, y is the blur image， τ is the regularization parameter.

Based on the SALSA variable segmentation， the equation (9)can be translated into:

$$\min_{x\in R^N, v\in R^N} \frac{1}{2}\| y-\Phi x\|_2^2 + \tau \| v \|_1 \quad s.t.\ \Psi x\text{-}v = 0 \qquad (10)$$

v is the corresponding frequency variable of spatial variables x. The equation (10) is sloved by using an augmented Lagrangian method.

$$\begin{pmatrix} x \\ v \end{pmatrix} \in \arg\min_{z} L(x,v,\lambda,\mu) = \arg\min_{x,v} \frac{1}{2}\| y-\Phi x\|_2^2 + \tau \| v\|_1 + \frac{\mu}{2}\| \Psi x - v - d \|_2^2 \qquad (11)$$

$\mu \geq 0$ is called the penalty parameter， $d \in R^N$ is the iterated variable which related to the Lagrange multiplier[6] , and updating by the following equation:

$$d_{k+1} = d_k - \Psi x_{k+1} + v_{k+1} \qquad (12)$$

d_{k+1} represents the $(\mathrm{k}+1)$th updating value of d, x_{k+1} is the $(\mathrm{k}+1)$th iterated spatial variable value, v_{k+1} is the $(\mathrm{k}+1)$th iterated frequency variable value.

Applying the alternating direction method of multipliers(ADMM)[18] to equation(11), which can be translated into the following form:

$$x_{k+1} \in \arg\min_{x} \frac{1}{2}\| y-\Phi x\|_2^2 + \frac{\mu}{2}\| \Psi x - v_{\mathrm{k}} - d_k \|_2^2 \qquad (13)$$

From the above two equations, we can see that x_{k+1} is obtained by v_k , meanwhile, v_{k+1} is obtained by the present x_{k+1}, that means, in the process of the iteration, the spatial and frequency variables are constraint for each other alternately to get the optimization solution respectively.

Applying the Sherman-Morrison-Woodbury (SMW)[19-20] matrix inversion to obtain the l_2 -norm optimization solution of spatial variable x. And the optimization solution of v is sloved by Soft threshold shrinkage.

$$v_{k+1} = soft((\Psi x_{k+1} - d_k), \tau/\mu) \qquad (14)$$

Finally ,the HR image reconstruction by MCSS_SR can be expressed as follows:

$$X_{MCSS\_SR} = \beta_{j_0}^{(X_{CS})}\varphi_{j_0} + \sum_{j=j_0}^{J}\sum_{d}\hat{\alpha}_{j,d}^{(X)}\phi_{j,d} \qquad (15)$$

IV. EXPERIMENTAL RESULTS AND ANALYSIS

In order to prove the validity of MCSS method established in Shearlet domain, Cameraman and Barbara images are chosen as the test images(of size 256×256).,then decomposed by DST, J is the total scale number, corresponding direction number of each scale $d_j = 2^j + 2$ .To ensure the subband information can be accurately recovered via MCSS, the measure time is shown in $m_{j,d} = C_1 \cdot \left(N_j / d_j \right) \cdot \tau \cdot \log\left(N_j\right)$,where C_1 is a constant, N_j is a certain subband dimention of the scale(the dimension is j identical for the subband in different directions but the same scale) . As known by the characteristics of LP decomposition in DST scale, $N_j = N \cdot 2^{-2(J-j)}$, τ is the sparse degree of image, assume $\tau = C_2 \cdot 10^{-(j+1)} \cdot d_j$ (C_2 is a constant). Set $J=3, C_1=4, C_2=2.5$, and $m_{j,d}$ is shown in Table 1.

Table 1 The corresponding $m_{j,d}$ of different scales

	N_j	d_j	τ	$m_{j,d}$
$j=0$	32×32	0	1	1024
$j=1$	64×64	4	$2.5\times10^{-2}\times4$	1479
$j=2$	128×128	6	$2.5\times10^{-3}\times6$	690

The total number of observations in MCSS is $M = m_0 + \sum_{j=1}^{J}\sum_{d} m_{j,d} \cdot d_j = 14240$ .Under the same M , we compare MCSS with traditional CS method[1] , the wavelet-based multi-scale compressed sensing (WBMCS) [4] and the Curvelet-based multi-scale compressed sensing (CBMCS)[3], in attempt to verify the validity of MCSS from the reconstructed image quality. The experimental results are shown in figure2.

Cameraman image | The image of Traditional CS PSNR=24.59 dB | The image of WBMCS PSNR=26.31 dB | The image of CBMCS PSNR=29.83 dB | The image of MCSS PSNR=33.05 dB

Barbara image | The image of Traditional CS PSNR=23.41 dB | The image of WBMCS PSNR=25.57 dB | The image of CBMCS PSNR=29.01 dB | The image of MCSS PSNR=32.35 dB

Figure.2 The image restoration results of four sparse representation applied to MCSS_SR

To verify the effectiveness of MCSS_SR method in super-resolution reconstruction based on CS, The images of Butterfly, Raccoon, Eye Test and the Girl are chosen as the ideal HR images(of sizes 256×256); Our work is compared with the compressive image super resolution (CISR) [21], image super resolution as sparse representation of raw image patches(SRSR) [22], in terms of the visual effect of the recovery image (as shown in figure 11), PSNR, RMSE and computation time respectively (as shown in table 2). The simulated experimental platform is Matlab7.1, and the frequency and memory of the computer are 3.01 GHz and 2 GB respectively. We first apply the down-sampling matrix **D** to the HR image and get the low resolution image of dimension $N^{(low)}=\frac{N}{n}=\frac{1}{4}\cdot(256\times256)=128\times128$;

To ensure a full observation, the observation times of each directional subband in LR image is $m_{j,d}=C_1\cdot n\cdot\left(N_j^{(low)}\big/d_j\right)\cdot\tau\cdot\log\left(N_j^{(low)}\right)$, then, the total sampling times of LR image is $M=13472$, and $\frac{M}{N^{(low)}}\approx0.82$, which means only by using about $4/5$ information of LR image, the corresponding HR image can be reconstructed in highly probability.

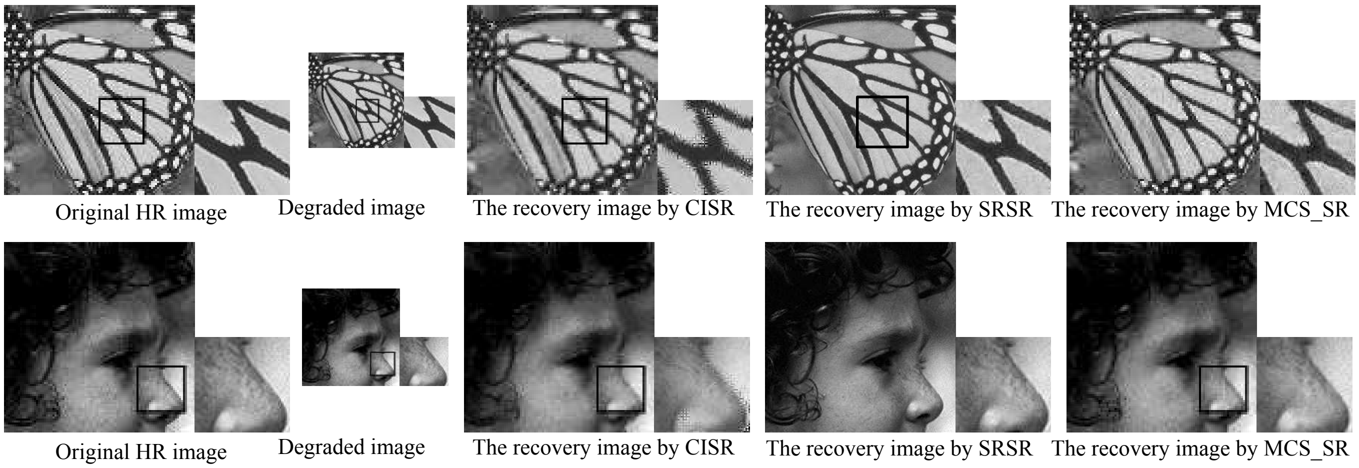

Figure.3 The image restoration results of three methods

As shown in figure 3, there is the “dot” noise in terms of the quality of the recovered image via CISR methods, which adopts orthogonal wavelet transform as sparse representation and wiener filter to smooth images. SRSR method, through establishing the relationship of sparse representation structure between HR and LR image blocks, can recover the image with more details, but due to the introduction of the overcomplete dictionary as a sparse representation, the whole method is highly complex. MCSS_SR method can recover most of image details with a slight noise. By compared with CISR method, the effect of the recovery image has improved greatly. By compared with SRSR method, although the texture details of the recovery image are slightly inferior, however, because of its low complexity, our work is obviously better than SRSR method in computational speed.

Table 2 The comparison of restoration results by three methods (The unit of PSNR is dB)

Image	**CISR**			**SRSR**			**MCSS_SR**		
	PSNR	**RMSE**	**Time**	**PSNR**	**RME**	**Time**	**PSNR**	**RME**	**Time**
Butterfly	27.41	29.74	9.7s	33.15	7.92	602s	32.72	8.75	31.4s
Raccoon	26.92	33.29	10.4s	31.40	12.68	614s	30.57	14.36	32.0s
Eyetest	28.01	25.90	9.1s	34.27	5.89	599s	33.12	7.68	29.8s
Girl	27.39	29.88	10.8s	32.83	10.44	619s	31.05	12.86	31.7s

From Table 2, we can see that the PSNR average value of recovery image in MCSS_SR is beyond 4.43dB and the RMSE average value reduces about 18.7 in comparison with CISR method. Besides, the two average values are a slightly 1.04dB lower and 1.68 higher than SRSR method. And the computation time of MCSS_SR and CISR is in the same order of magnitude while about 600 seconds in SRSR method. So MCSS_SR will not increase the computational complexity and is suitable for super-resolution reconstruction in actual system.

To test the super-resolution reconstruction property of MCSS_SR method, we set the digital camera resolution up to 300000 pixels to obtain the live action images named Building, Library and Teaching Building respectively(of size 640×480). The test LR images are regarded as clear ones without noise and blur phenomena, to ensure it can verify accurately the effectiveness of MCSS_SR- based SR reconstruction algorithm. Assume the amplification factor $\gamma = 2$, and the size of reconstructed images is 1280×960.In order to see to the accuracy of measurement, we set measurement times $M = 25$ ten thousand times. Figure 4 represents the image effect of MCSS_SR based super resolution reconstruction.

As shown in figure 4, the recovered HR images by using bilinear interpolation method are unable to identify. And the reconstructed image effect by MCSS_SR is obviously better than the ones of directly amplified image, although it is not as good as the images via 1.3 million camera, the observations is only 0.2 times of the former, so it can effectively save sampling and transmission power consumption of the system.

To test the effectiveness of MCSS in MCSS_SR, we compare it with CS_SR method in terms of the reconstructed image quality. The images of EyeTest and Raccoon (of size 256×256) are chosen as the test images. And measurement times $M = 14240$ is set for each method. Figure 5 represents the recovery effect of EyeTest and Raccoon images. From figure 5, we can see that the black box area reflects the obvious difference in image details between the traditional CS_SR and MCSS_SR. The effect of reconstructed images drops sharply with strong and insufficient LR image details. With this MCSS_SR method, it can recover subtle details of images to maximum extent due to the fact that in CS theory, the sparser of the signal, the better recovery effect to get.

From the Eyetest image, we can see that the reconstructed image by MCSS_SR has slight noise and artifact phenomenon in the white area; each subband reconstruction can generate a slight error, which is, after iteration, ultimately reflected in the form of noise and artifact in the recovery images. Nonetheless, it is still excellent for the recovery image effect by MCSS_SR.

From figure 6, it can be seen that the average PSNR value of MCSS_SR method is about 2.53 dB higher than that of traditional CS while the computation time decreases about 10.9s. Thus, compared with CS_SR method, the MCS in MCSS_SR increases reconstruction times， but for the sparse signal, there is no need to have sparse representation during the iteration, and it is considered that our work does not overly increase the system complexity, and the reconstruction speed remains at the same order of magnitudes. Since reconstruction image quality of MCSS_SR method is obviously better than that of CS_SR, it is reasonable to sacrifice a little time to obtain more ideal recovery images.

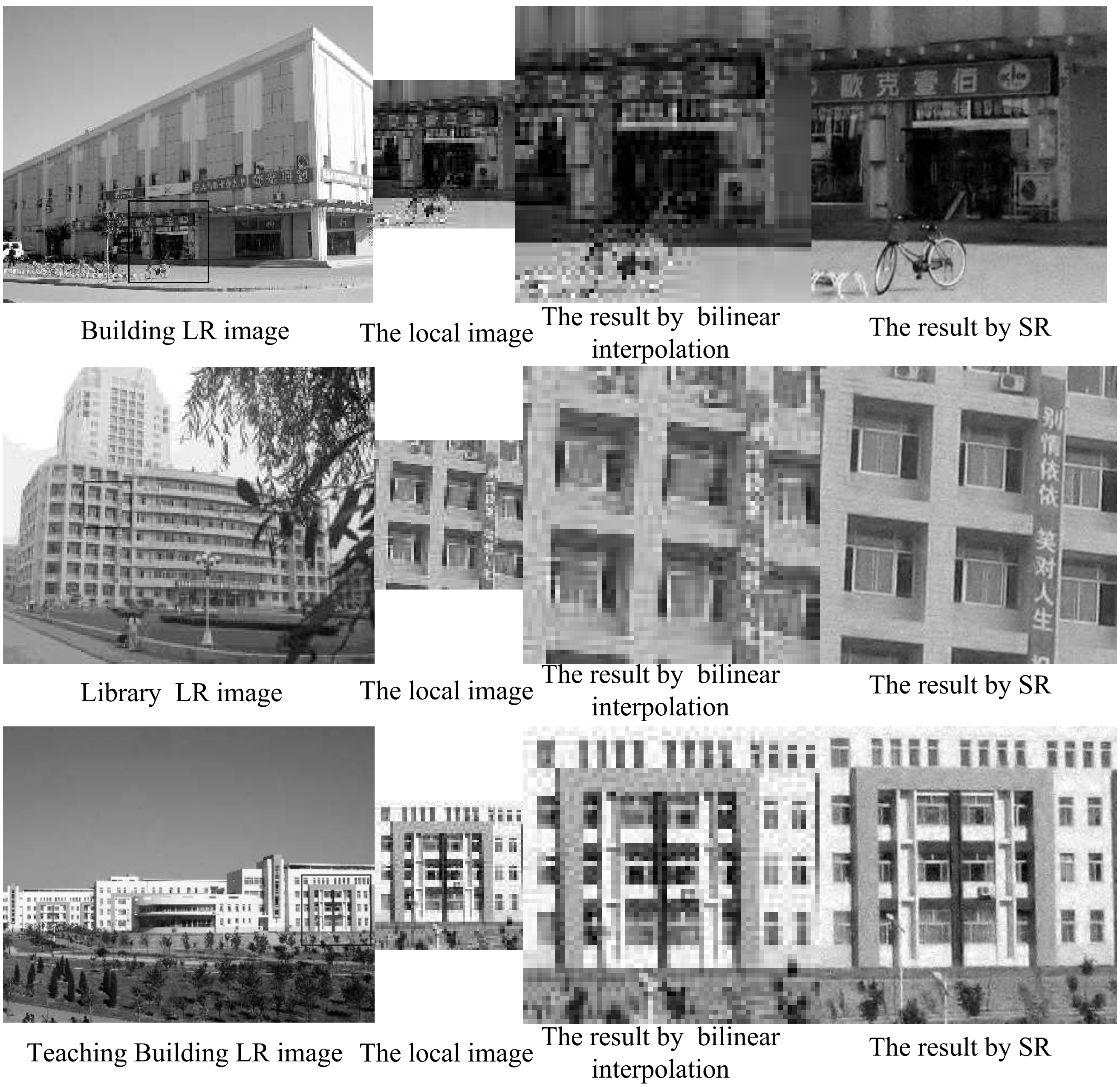

Figure.4 The amplified results of two methods

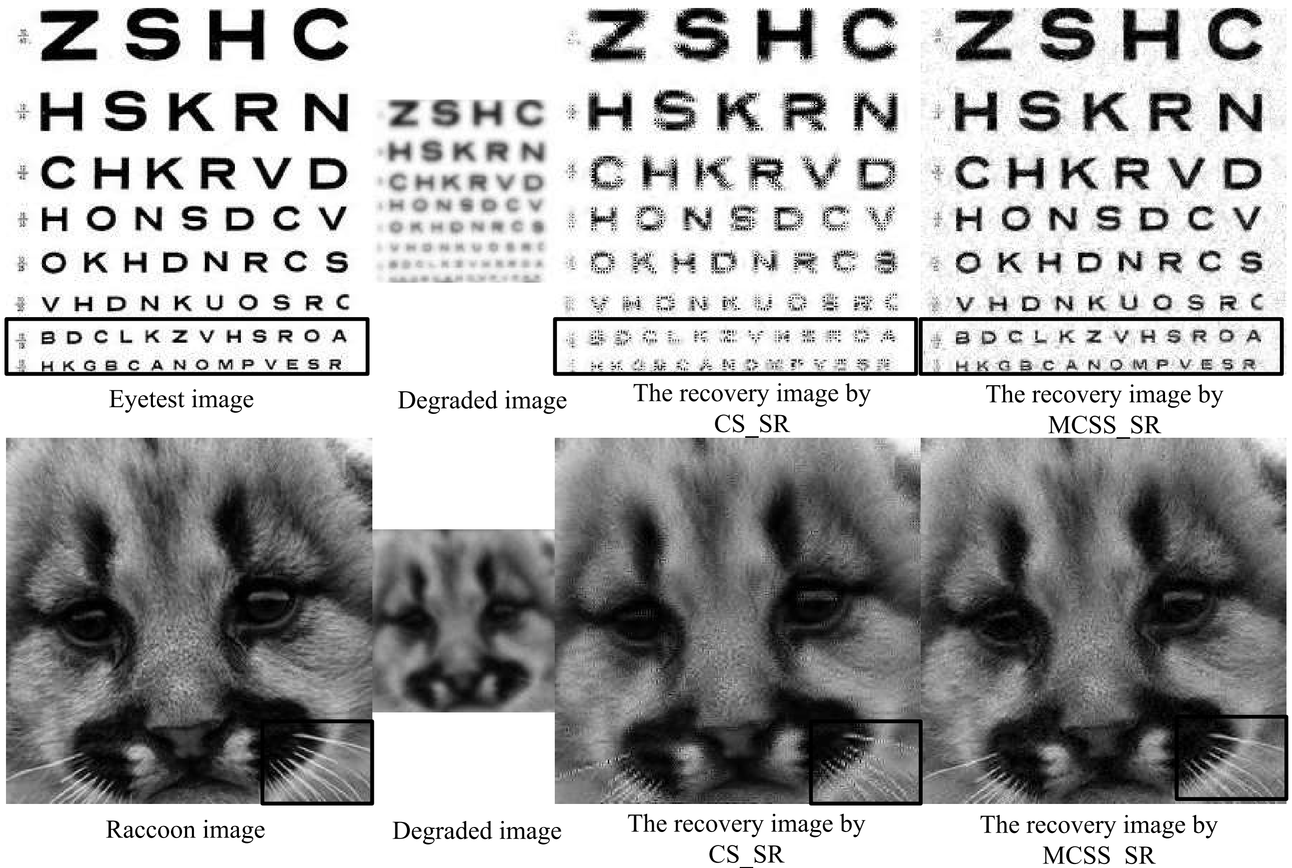

Figure.5 The image restoration results of CS_SR and MCSS_SR methods

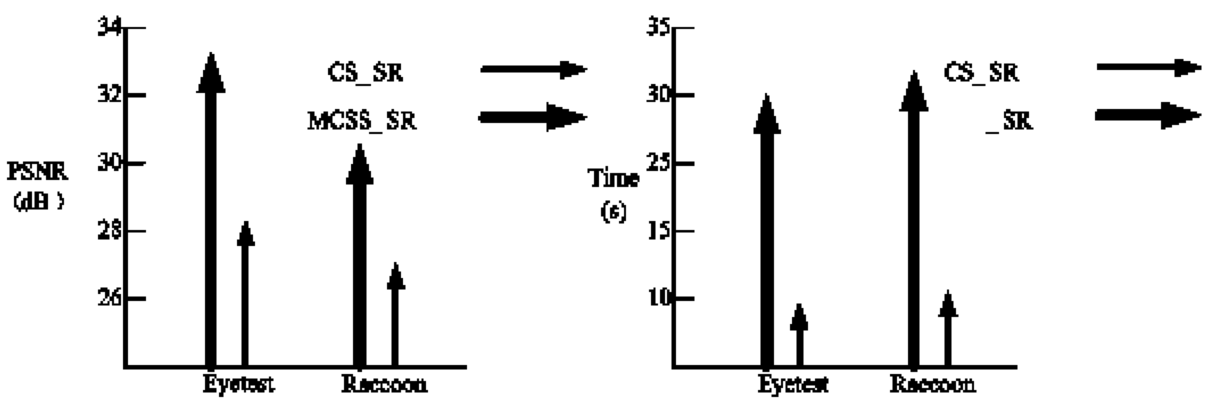

Figure.6 The value of PSNR and time comparison of image restoration results of CS_SR and MCSS_SR methods

(a) TwIST (PSNR=27.69dB)　　(b) FISTA (PSNR=26.95dB)　　(c) SALSA (PSNR=26.42dB)

Figure.7 The local reconstruction image of Lena at the sampling rate of 30%

(a) TwIST　　(b) FISTA　　(c) SALSA　　(

PSNR=33.80dB)　　(PSNR=34.12dB)　　(PSNR=35.26dB)

Figure.8 The local reconstruction image of Bone at the sampling rate of 30%

We evaluate the performance of SALSA, two-step iterative shrinkage- thresholding (TwIST)[23] and fast iterative shrinkage-thresholding algorithm (FISTA)[24] for image reconstruction. we choose the standard images of Lena,Barbara and the medical image of Bone as the test image. And set $\tau = 0.001\times\max(\Phi^T y)$, $\mu = 0.1\times\tau$ .figure 7 and figure 8 are the local reconstruction images of Lena and Barbara at the sampling rate of 30%. From the figures, we can see that the reconstructed image of our work persist more details than other two algorithms, The PSNR value also is improved.

Table 3 shows the comparison of PSNR values and computation time of two test images at different sampling radios. From Table 1,we can see that the difference between our scheme and other methods is dramatic, for example, when the sampling rate of Lena image is set to 30% , the PSNR values of our scheme is higher than TwIST and FISTA by 1.24 dB and 1.89 dB. Meanwhile the computation time is reduced by our algorithm, which means our scheme can achieve good reconstruction results only using less time and therefore saves energy needed.

Table 3. The comparison of PSNR value and computation time of four algorithms at different sampling radios

	Algorithms	**The sampling radios**							
		10%		**20%**		**30%**		**40%**	
		PSNR	*Time*	*PSNR*	*Time*	*PSNR*	*Time*	*PSNR*	*Time*
Lena	TwIST	24.00	8.38	26.44	11.51	27.92	12.73	28.51	16.24
	FISTA	19.31	9.79	24.49	9.04	27.27	9.26	28.07	9.95
	SALSA	18.40	8.07	24.16	7.90	26.16	8.92	26.88	9.05
	Modified SALSA	26.08	6.52	27.92	5.95	29.16	6.18	30.18	7.23
Barbara	TwIST	24.57	8.89	26.92	10.17	28.73	12.92	29.15	16.04
	FISTA	19.57	9.35	25.36	9.14	27.75	10.25	28.93	9.98
	SALSA	18.71	7.57	24.11	7.45	26.19	6.99	26.37	7.89
	Modified SALSA	26.32	6.34	28.34	6.67	29.61	6.03	30.38	6.56

V. **CONCLUSIONS**

In MCSS_SR, the MCSS constructed in Shearlet domain can effectively reduce the sampling value while guarantee the quality of reconstructed images. The improved measurement matrix via down-sampling and blur operators satisfies the requirement of RIP.And SALSA can speed up the convergence, meanwhile preserve more details in the process of reconstruction. the Experimental results have proved that MCSS_SR advantages at computation time and the quality of reconstructed images.

REFERENCES

[1] Donoho D L, “Compressed sensing”, IEEE Transactions on Information Theory, vol. 52, No. 4, 2006, pp. 1289-1306.

[2] Daode Zhang,Yangliu Xue,Xuhui Ye , Yanli Li,"Research On Chips' Defect Extraction Based On Image-matching ", International Journal on Smart Sensing and Intelligent Systems (S2IS), Mar 10. 2014, pp. 321-336.

[3] Tsaig Y, Donoho D L, "Extensions of compressed sensing", Signal Processing,vol. 86, No. 3,2006, pp. 533-548.

[4] James E. Fowler, Sungkwang Mun, and Eric W. Tramel,"Multi-scale block compressed sensing with smoothed projected landweber reconstruction", 19th European Signal Processing Conference, Barcelona, Spain,2011.

[5] Feng LUO , Fengjian HU,"A Comprehensive Survey Of Vision Based Vehicle Intelligent Front Light System",International Journal on Smart Sensing and Intelligent Systems (S2IS), June 1. 2014, pp. 701-723.

[6] Pu Jian,Zhang Junping," Super-Resolution through Dictionary Learning and Sparse Representation" ,[J].pattern recognition and artificial intelligence, 2010,pp. 335-340.

[7] Guohui Wu, Xingkun Li, Jiyang Dai."Improved Measure Algorithm Based On CoSaMP For Image Recovery ",International Journal on Smart Sensing and Intelligent Systems (S2IS), June 1. 2014, pp. 724-739.

[8] Candes E, Romberg J,"Sparsity and incoherence in compressive sampling",[J]. Inverse Problems, vol. 23, No. 3, 2007, pp. 969-985.

[9] Ahadul Imam, Justin Chi, Mohammad Mozumdar,"Data Compression And Visualization For Wireless Sensor Networks ",International Journal on Smart Sensing and Intelligent Systems (S2IS),Dec 1. 2015, pp. 2083- 2115.

[10] Payman Moallem1,"Compensation Of Capacitive Differential Pressure Sensor Using Multi Layer Perceptron Neural Network", International Journal on Smart Sensing and Intelligent Systems (S2IS), Sep 1. 2015, pp. 1443-1463.

[11] M. Afonso, J. Bioucas-Dias, M. Figueiredo, "Fast image recovery using variable splitting and constrained optimization",[J]. IEEE Transactions on Signal Processing, vol. 19, No. 9, 2010, pp. 2345-235.

[12] Guo K and Labate D, "Optimally Sparse multidimensional representation using shearlets ",SIAM J.Math. Anal, Vol. 39, 2007, pp. 298-318.

[13] Easley G, Labate D, Lim W."Sparse Directional image representations using the discrete Shearlet transform", [J].Applied and Computational Harmonic Analysis, vol. 25 ,2008, pp. 25-46.

[14] Do T T, Tran T D, Lu G, “Fast compressive sampling with structurally random matrices” Proceedings of the IEEE International Conference on Acoustics, Speech and Signal Processing. Washington D C: IEEE Computer Society Press, 2008, pp. 3369-3372.

[15] Chen SSB, Donoho D L, M A Saunders, “Atomic decomposition by basis pursuit”, [J]. SIAM Journal on Scientific Computation, vol. 20, No. 1, 1998, pp. 33-61.

[16] Tropp J A. Greed is good, ”Algorithmic results for sparse approximation” ,[J]. IEEE Transactions on Information Theory, vol. 50, No. 10, 2004, pp. 2231-2242.

[17] Blumensath T, Davies M E, ”Normalised iterative hard thresholding:guaranteed stability and performance”,[J],IEEE Journal of Selected Topics in Signal Processing, vol. 4, No. 2,2010, pp. 298-309.

[18] Wenqing Chen, 2 Tao Wang and 3 Bailing Wang, ”Design Of Digital Image Encryption Algorithm Based On Mixed Chaotic Sequences” International Journal on Smart Sensing and Intelligent Systems (S2IS), Dec. 1. 2014, pp. 1453-1469.

[19] Yongqing Wang1* and Xiling Liu, ”Face Recognition Based On Improved Support Vector Clustering ”,International Journal on Smart Sensing and Intelligent Systems (S2IS), Dec. 1. 2014, pp. 1807-1829.

[20] Qu Xiao-Bo, Yan Jing-Wen, Zhu Zi-Qian, Chen Ben-Gang. “Multipulse coupled neural networks”. In Proceedings of International Conference on Bio-Inspired Computing Theories and Applications. Zhengzhou, China: Publishing House of Electronics Industry. 2007,pp.563-565.

[21] Sen P,Darabi S,”Compressive image super-resolution”, Proceedings of Signals, Systems and Computers. Los Alamitos:IEEE Computer Society Press,2009,pp. 1235-1242.

[22] Yang C, Wright J, Huang T, Ma Y ,”Image super-resolution via sparse representation”,[J].IEEE Trans. Image Process, vol. 19, No. 11, 2010.pp. 2861-2873.

[23] J. Bioucas-Dias, M. Figueiredo,“A new TwIST: Two-step iterative shrinkage/thresholding algorithms for image restoration”, [J]. IEEE Transactions on Image Processing, vol. 16, No. 12, 2007, pp. 2992-3004.

[24] A. Beck, M. Teboulle,”A fast iterative shrinkage-thresholding algorithm for linear inverse problems”, [J]. SIAM Journal on Imaging Sciences, vol. 2, No. 1, 2009, pp. 183-202.